Modeling subharmonic and chaotic ferroresonance with transformer core model including magnetic hysteresis effects

PAUL MOSES, MOHAMMAD MASOUM
Curtin University of Technology
Department of Electrical and Computer Engineering
Perth, WA, 6845
AUSTRALIA
paul.s.moses@gmail.com m.masoum@curtin.edu.au

Abstract: Ferroresonance is a highly destructive power quality phenomenon caused by complex oscillations generated by nonlinear magnetizing inductances in ferromagnetic materials and capacitive elements in power systems. In an effort to better understand ferroresonance and predict bifurcations and responses, an improved nonlinear transformer model for dynamic and steady-state operating conditions is developed which includes magnetic hysteresis nonlinearities of the transformer core. The model expands on Tellinen's scalar hysteresis approach which includes major and minor hysteresis loop effects. This paper carries out an investigation into single-phase transformer ferroresonance initiated by switching transients using the developed model. A range of ferroresonance modes (e.g., subharmonic and chaotic) initiated by switching transients is identified with the transformer core model. The model is used to compute time-domain waveforms of transformer flux, voltage and magnetizing current for several ferroresonance modes. Furthermore, Poincaré and phase-plane portraits are used to examine the stability domain of observed ferroresonance modes. The main contribution of this work is a new analysis into ferroresonance through an improved transformer model which incorporates magnetic hysteresis effects.

Key–Words: Chaos, ferroresonance, hysteresis model, nonlinear dynamics, Poincaré, power quality, transformer.

1 Introduction

Ferroresonance in power networks involving nonlinear transformers and capacitors has been well researched for nearly a century. However, it is only in recent years that nonlinear transformer modeling techniques have begun to approach the level of sophistication required for accurate ferroresonance studies which was mainly driven by developments in modern computing and simulation software. To that end, the importance of hysteresis nonlinearities in dynamic and transient simulation studies and its impact on the stability domain of ferroresonance modes has recently been demonstrated [1–4].

Ferroresonance can be understood as a complex oscillatory energy exchange between magnetic field energy of nonlinear magnetizing inductances of transformer/reactor cores and electric field energy of nearby capacitances (e.g., series compensated lines or circuit breaker grading capacitors). Without adequate dissipation through normal loads and losses, a substantial amount of energy sloshes back and forth within a power system and manifests as over-voltages and currents exhibiting high levels of distortion. The distortions can cause large losses in power systems and increase thermal stresses in transformers [5]. Several cases where significant equipment damage has occurred due to ferroresonance have been documented and continues to be a large safety hazard [6–8].

Over the years, research in ferroresonance has concentrated into three main areas: (1) improving analytical methods and transformer models, (2) development of transformer protection and mitigation strategies and (3) case studies of system level impacts [9, 10]. Despite the extensive literature available in this area, ferroresonance continues to be a challenging problem to analyze, predict and understand due to its highly nonlinear and dynamic behavior. Researchers must adopt complex mathematical notions such as chaos theory to gain insight into this phenomenon [11–13].

The four generally accepted ferroresonance modes which can occur are (1) fundamental ferroresonance (period-1), (2) subharmomic ferroresonance (e.g., period-3), (3) quasi-periodic ferroresonance and (4) chaotic ferroresonance. The last two are non-periodic modes. There is also the possibility of mixed modes or unstable modes where gradual system variations or perturbations cause sudden jumps (known as bifurcations [14]) from one mode to another [15, 16]. From a purely mathematical standpoint, these modes

are due to multiple competing solutions (known as attractors) to a system of nonlinear differential equations of an electromagnetic circuit. The nonlinearity is due to the magnetic properties of ferromagnetic material. Therefore, it is imperative to develop accurate nonlinear electromagnetic models for transformer cores to fully depict dynamic disturbances such as ferroresonance.

In this paper, a single-phase transformer model including hysteresis nonlinearities is developed to study possible ferroresonance behavior (e.g., subharmonic and chaotic modes). The model is used to generate ferroresonance conditions and plot resulting time-domain waveforms including flux, voltages and magnetizing currents, as well as Poincaré and phase-plane diagrams for selected values of series and shunt capacitors initiated by switching. Section II discusses the importance of hysteresis modeling and past contributions in this area. Section III provides an overview of some of the applied analytical techniques for studying dynamic and chaotic phenomena such as ferroresonance. The development of the transformer model with nonlinear magnetic hysteresis implementation is discussed in Section IV. Simulations results with discussion and the conclusions of this paper are provided in Sections V and VI.

2 Hysteresis Core Modeling

The modeling of hysteresis has evolved significantly since the 1970s when digital nonlinear core models were first being developed. Early modeling attempts indirectly incorporated hysteresis by the use of single-value nonlinear inductors in parallel with a resistor representing eddy-current and hysteretic losses. Models evolved to use families of ascending and descending curve functions for the inclusion of major and minor loop effects of ferromagnetic material. Some authors ignore minor loops and focus only on major loops or make use of scaling factors on major hysteresis loops to derive the minor loops. These nonlinear approximations are typically based on piece-wise, hyperbolic, trigonometric or differential equations. References [17, 18] provide a thorough historical review of progress in hysteresis modeling.

In addition to the mathematical complexity usually accompanying most hysteresis models, characterizing the core behavior from measurements can be quite challenging. For example, the well renowned Preisach-based hysteresis model [19] requires a set of first order descending curves of minor hysteresis loops to be measured. Another popular model by Jiles-Atherton [20] requires five fitting parameters to be determined by tedious and often imprecise measurements. The approach shown in this paper greatly simplifies core identification by adopting Tellinen's hysteresis model [21] which requires only the major hysteresis loop to be measured. The minor loops are dynamically estimated through mathematical relationships derived in Section IV.

Despite the existence of hysteresis models, there is still a tendency for transformer power quality studies to ignore hysteresis and use anhysteretic approximations of the $B - H$ characteristic because of the modeling complexity and computational burden associated with hysteresis nonlinearities. This simplification can be justified for some studies because transformer design has improved over the years and hysteresis loop widths have narrowed significantly to appear almost anhysteretic. Therefore, for steady-state power quality studies such as harmonic power flow in nonlinear transformers, single-valued anhysteretic functions are considered acceptable [22–26].

On the other hand, for the study of dynamic, transient and nonsinusoidal power system behavior, the representation of minor hysteresis loop trajectories becomes important as additional operating points are created by the dynamic disturbances imposed on a nonlinear hysteretic core model. This is especially true in ferroresonance where major and minor loop trajectories can potentially generate more ferroresonant operating points expanding the stability domain [3]. For this paper, a suitable nonlinear hysteretic core model of a single-phase transformer is developed to study ferroresonance.

3 Nonlinear Dynamical Systems

It is important to understand that many oscillatory modes of operation are possible for the same set of system parameters due to sensitivity to initial conditions and transients [27]. This can excite a system with transformer magnetizing inductances and capacitances into many different steady-state and chaotic ferroresonance oscillatory modes. This fact is true for modern power systems because variations in circuit breaker operating times on the point of wave in ac cycle, random switching events and residual fluxes are all variable initial conditions impacting how and which ferroresonance mode(s) occur. In lieu of these complexities, new mathematical analytical techniques have been developed to understand this behavior.

Kieny and Mork first proposed the connection between ferroresonance and nonlinear dynamical systems and chaos theory in subsequent publications originating from the late 1980's [11–13]. Since then, this approach is now considered the most appropriate mathematical framework for studying the many com-

plex ferroresonance modes that can exist in a power system. Performing time and frequency-domain analysis alone does not provide adequate insight into this phenomenon. Phase-plane portraits and Poincaré mapping are two popular analytical approaches.

Phase-plane diagrams are most useful for characterizing the time evolution of ferroresonance modes. For a given system state variable x (e.g., transformer voltage), the time derivate of this variable $\dot{x}(t)$ is plotted against the variable magnitude $x(t)$ and traced out in time. Resulting trajectories can be interpreted for useful insight into the time evolutionary behavior of a nonlinear dynamical system. The phase-plane representation can be simplified to what is known as a Poincaré map. This is achieved by sampling the state variable at the power system frequency (e.g., 50 Hz) and plotting the phase-plane diagram 'stroboscopically' in phase space. These visual representations are very useful in classifying and distinguishing different ferroresonance modes and features. Reference [15] provides a good introduction to interpreting these diagrams. In this paper, these techniques are applied with the proposed nonlinear transformer model to demonstrate different ferroresonance conditions.

4 Proposed Single-Phase Transformer Core Model with Hysteresis Nonlinearity

A PSPICE computer model was developed for a single-phase transformer with hysteresis nonlinearities (Fig. 2). A scalar hysteresis model based on [21] is implemented for this work due to its simplicity in implementation for circuit simulation. The magnetic flux density b and field intensity h are the main parameters for this model. However, for this paper, the hysteresis equations are modified such that flux linkages and magnetizing currents are computed instead of b and h (i.e., $b \rightarrow \lambda$ and $h \rightarrow i_m$). These parameters are more accessible in PSPICE and easily measured from laboratory measurements. The modified hysteresis equations are as follows:

$$\frac{di_m}{dt} = \frac{d\lambda}{dt} \cdot \frac{1}{L_0 + \frac{\lambda_-(i_m)-\lambda(i_m)}{\lambda_-(i_m)-\lambda_+(i_m)}\left(\frac{d\lambda_+(i_m)}{di_m} - L_0\right)} \quad \text{if } \frac{d\lambda}{dt} \geq 0$$

$$\frac{di_m}{dt} = \frac{d\lambda}{dt} \cdot \frac{1}{L_0 + \frac{\lambda(i_m)-\lambda_+(i_m)}{\lambda_-(i_m)-\lambda_+(i_m)}\left(\frac{d\lambda_-(i_m)}{di_m} - L_0\right)} \quad \text{if } \frac{d\lambda}{dt} < 0 \tag{1}$$

where λ_+, λ_- and λ are the limiting ascending and descending curve functions and instantaneous flux linkages, respectively, dependent on magnetizing current i_m. L_0 is the inductance or slope in the saturated region along the limiting hysteresis curves. As noted from (1), the basis for this model is the use of slope functions for λ_+ and λ_- to compute magnetization processes. This is derived directly from magnetics theory with the assumption that domain wall motion density (Barkhausen jumps) are proportional to the growth of domain regions which increase with magnetic field strength [21].

The flux linkage and current relationships for the hysteresis model are

$$e(t) = \frac{d\lambda(t)}{dt} \tag{2}$$

$$i(t) = i_m(t) + i_c(t) \tag{3}$$

Before equation (1) can be computed, the ascending and descending limiting hysteresis loop segments must be specified. This paper proposes nonlinear analytical expressions to describe the ascending (λ_+) and descending (λ_-) limiting hysteresis loop segments. The proposed nonlinear function (4) can accurately be fitted to measured $\lambda - i$ characteristics of a real nonlinear transformer.

$$f(i_m) = \text{sgn}(i_m) \cdot \alpha \log_e(\beta |i_m| + 1) \tag{4}$$

The fitting parameters α and β control the vertical and horizontal scaling. The ascending limiting loop segment is derived from (4) by shifting the function $f(i_m)$ to the right by an increment of σ and similarly the descending loop function is obtained by shifting the function to the left by σ (eqs. (5)-(6), Fig. 1). Effectively, σ controls the width of the limiting hysteresis loop.

$$\lambda_+(i_m) = f(i_m - \sigma) \tag{5}$$

$$\lambda_-(i_m) = f(i_m + \sigma) \tag{6}$$

The slope of the above ascending and descending functions must be computed before the modified hysteresis equations (1) can be computed. The ascending and descending slope functions $\frac{d\lambda_\pm(i_m)}{di_m}$ are derived through differentiation of (5)-(6) with respect to magnetizing current.

$$\frac{d\lambda_\pm(i_m)}{di_m} = \frac{\alpha\beta}{\beta |i_m \mp \sigma| + 1} \tag{7}$$

Equation (1) is then computed from substitution of (2), (5), (6) and (7). The next step is for the program

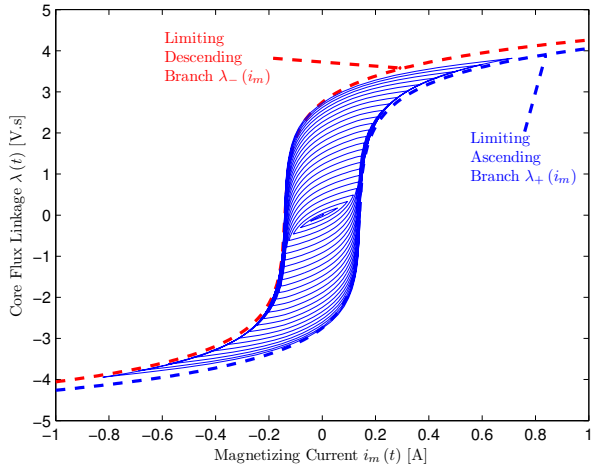

Figure 1: The developed hysteresis model is shown under ramped sinusoidal excitation to demonstrate the capability of the model to form major and minor hysteresis loops constrained by ascending (λ_+) and descending (λ_-) limiting hysteresis curve functions.

to select one of the two equations (1) for $\frac{di_m}{dt}$ based on whether the magnetization is increasing or decreasing. An IF statement in PSPICE is used to select one of the two equations in (1) based on the sign of the induced voltage (2). The magnetizing current i_m is evaluated by integrating (1).

There are two approaches to realize the above expressions in a PSPICE circuit. The first method is to implement a controlled voltage source for the induced voltage (2) based on (1). The second approach is more abstract but more numerically stable and is thus the favored approach. Equation (1) is realized by implementing a circuit loop consisting of an arbitrary capacitor with inherent current and voltage relationship together with a controlled current source (Fig. 2).

$$i = C\frac{dV}{dt} = 1 \cdot \frac{d\lambda}{dt} \tag{8}$$

The capacitor voltage is in fact the flux linkage and its current is governed by the controlled current source based on (1). A large resistance ($10^{12}\ \Omega$) is placed in parallel with the capacitor to suppress numerical convergence and floating node problems. The developed hysteresis model can form major and minor hysteresis loops based on specified λ_+ and λ_- functions. This is demonstrated in Fig. 1 for linearly increasing sinusoidal excitation. The completed electric circuit transformer model with hysteresis equations is processed in time-domain through PSPICE's variable step Newton-Raphson algorithm and nonlinear equations are solved iteratively.

5 Simulation Results

This section applies the developed nonlinear transformer core model with hysteresis to identify possible ferroresonance modes generated by series switching (e.g., circuit breaker action) with different shunt and series capacitances. The transformer model is based on a real single-phase 440/55 V 50 Hz laboratory transformer. The winding and core-loss impedances have been determined by open and short circuit tests ($R_s = 9.4\,\Omega$, $L_s = 6.34$ mH, $R_c = 14\,k\,\Omega$). The magnetization hysteresis loop characteristic ($\lambda - i_m$) has been measured by exciting the transformer primary with twice the rated excitation voltage and integrating the corresponding induced secondary voltages to estimate core flux. The hysteresis model parameters have been adjusted to match the measured hysteresis loop using curve fitting techniques (see Appendix).

The scenario under investigation is an unloaded single-phase transformer operating under steady-state conditions interrupted by a switch which is opened at $t = 0.1$s. This case is representative of single-phase fuse or circuit breaker action resulting in a series ferroresonance circuit as shown in Fig 2. This can also occur for three-phase transformer banks (i.e., 3 single-phase transformers) where one of the phases has developed a fault and the circuit breaker has opened. In a generalized way, to account for various capacitance sources as previously mentioned, the impact of different combinations of series and shunt capacitances (C_{series}, C_{shunt}) are investigated.

5.1 Subharmonic Ferroresonance Modes

Fig. 3 demonstrates period-3 type ferroresonance initiated by the opening of the switch at $t = 0.1$s when C_{series} and C_{shunt} are set to 10 and $38\,\mu F$, respectively. The flux and voltage waveforms indicate the transformer becoming highly saturated with excessive magnetizing currents and sustained harmonic distortions. The phase-plane and Poincaré diagrams indicate the system settling to a stable attracting (and distorted) limit cycle. To demonstrate the different wave shapes that are possible for the same type of ferroresonance mode, another type of period-3 ferroresonance is shown for $C_{series} = 18.2\,\mu F$ and $C_{shunt} = 29.1\,\mu F$ (Fig. 4). The resulting oscillations for this case result in asymmetrical core saturation as indicated by the magnetizing currents and computed hysteresis loop (Fig.4c).

For C_{series} and C_{shunt} set to 10 and $22\,\mu F$, harmonic distortions have increased for flux and voltage waveforms (Fig. 5). Furthermore, the transient period from normal operation to ferroresonance has a longer duration compared to the previous case. The

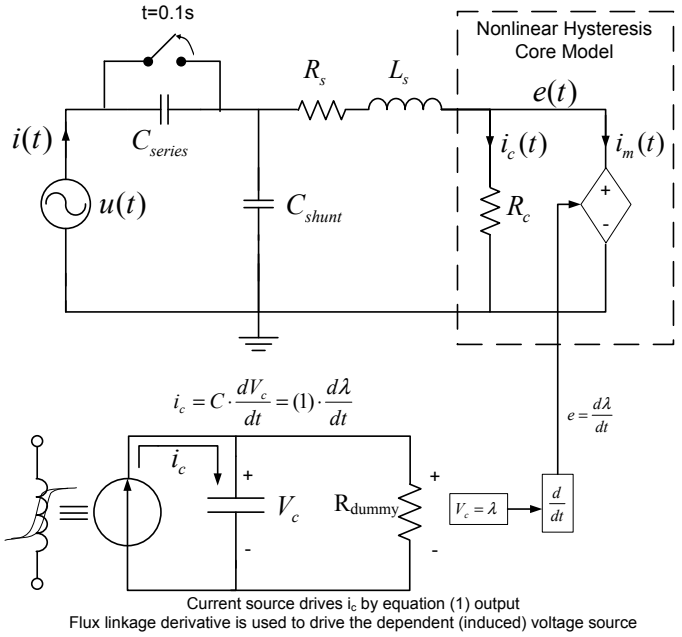

Figure 2: Ferroresonance circuit in a nonlinear transformer with dynamic magnetic hysteresis core model

group of five dots in the Poincaré map indicate this is to be period-5 type ferroresonance. The phase-plane diagram suggests the presence of competing cyclical attractors in the stability domain.

Similarly, with C_{series} and C_{shunt} are set to 29 and $38\,\mu F$, respectively, the switching action causes the transformer to exhibit extremely distorted period-7 type ferroresonance voltages (Fig. 6). The impact on hysteresis loop formation is more pronounced and is shown in Fig. 6c.

To emphasize the sensitivity of this phenomenon to a small change in a system parameter, C_{series} is varied by a small amount from the previous case to $28\,\mu F$ and the simulation is repeated (Fig. 7). The resulting waveforms show unstable ferroresonance modes which appear to be period-3 type lasting for only a few cycles before dampening out. It is interesting to observe that due to the flux and voltage relationship (2), the flux waveform takes a long time to stabilize compared to the voltage waveform.

In general, it was observed that most of the observed oscillations throughout this study were of the subharmonic type as shown. This is consistent with the findings of Lamba *et al.* [4] which concluded that hysteresis nonlinearities will lead to expanded subharmonic modes in the stability domain. However, in that that study some bifurcations to fundamental ferroresonance (period-1) were observed which was not the case in this analysis. Even after a rigorous search, no fundamental ferroresonance could be identified. This does not necessarily preclude the existence of period-

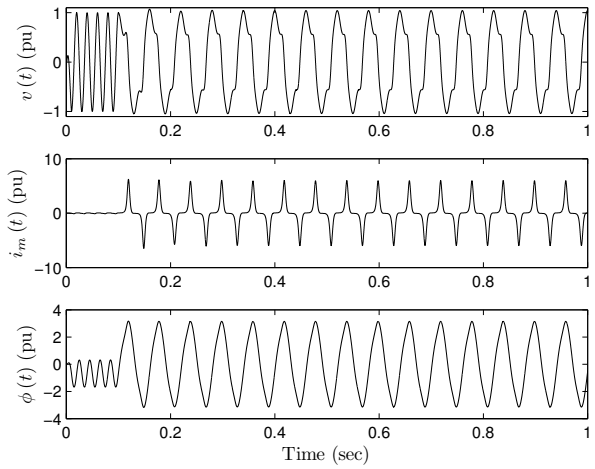

(a)

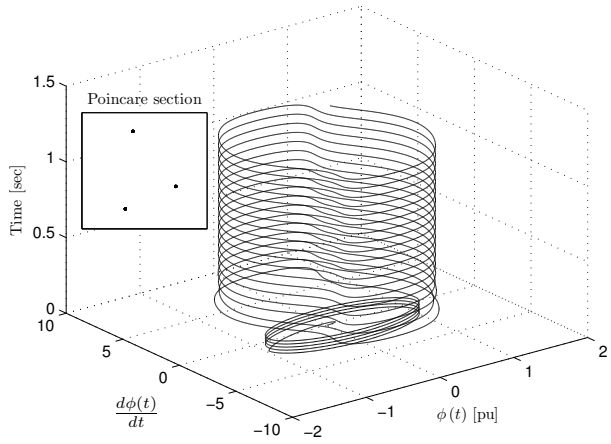

(b)

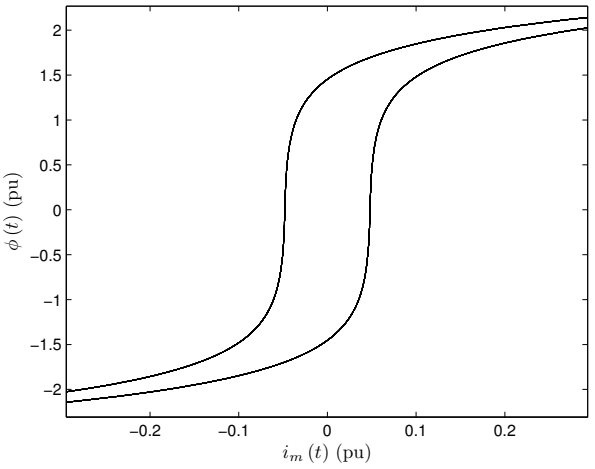

(c)

Figure 3: Subharmonic ferroresonance (Period-3) occurring at $C_{series} = 10\,\mu F$ and $C_{shunt} = 38\,\mu F$; (a) time-domain waveforms for flux, magnetizing current and voltage, (b) Poincaré and phase-plane diagrams, and (c) steady-state core hysteresis formation.

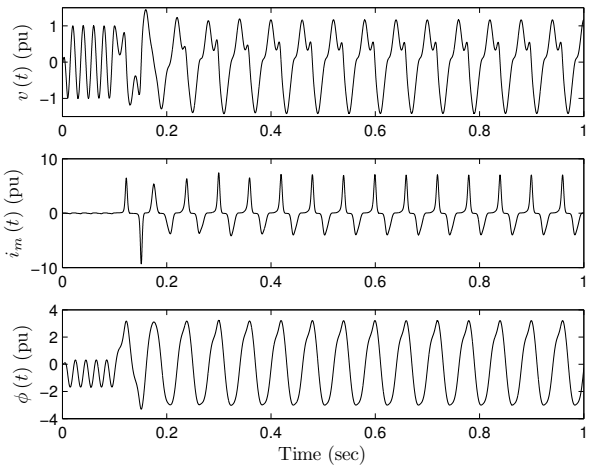

(a)

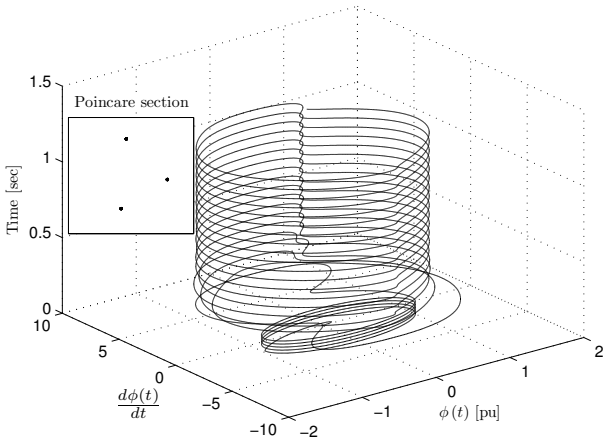

(b)

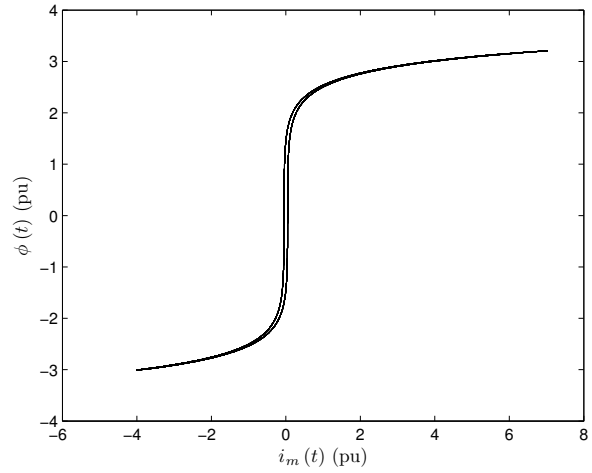

(c)

Figure 4: Subharmonic ferroresonance (Period-3) occurring at $C_{series} = 18.2\,\mu F$ and $C_{shunt} = 29.1\,\mu F$; (a) time-domain waveforms for flux, magnetizing current and voltage, (b) Poincaré and phase-plane diagrams, and (c) steady-state core hysteresis formation.

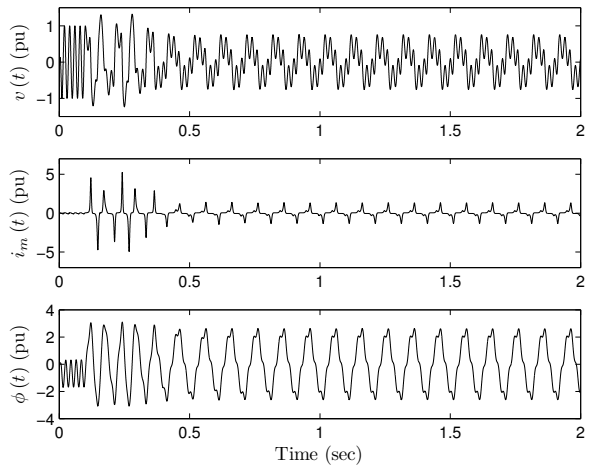

(a)

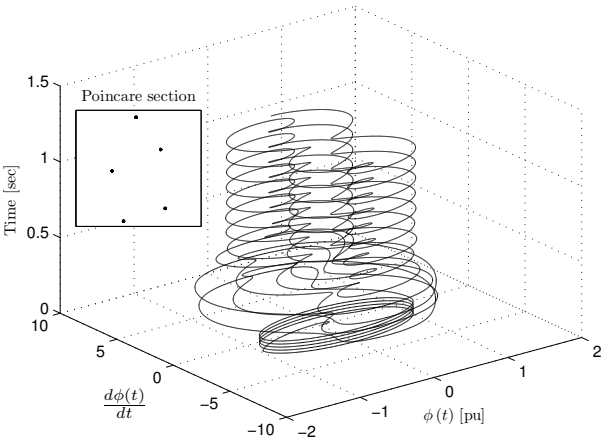

(b)

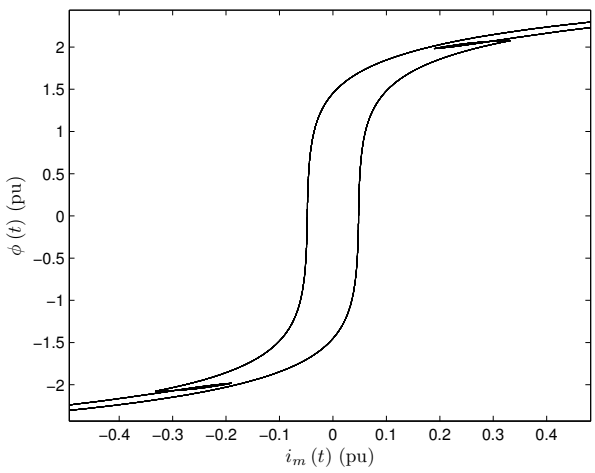

(c)

Figure 5: Subharmonic ferroresonance (Period-5) occurring at $C_{series} = 10\,\mu F$ and $C_{shunt} = 22\,\mu F$; (a) time-domain waveforms for flux, magnetizing current and voltage, (b) Poincaré and phase-plane diagrams, and (c) steady-state core hysteresis formation.

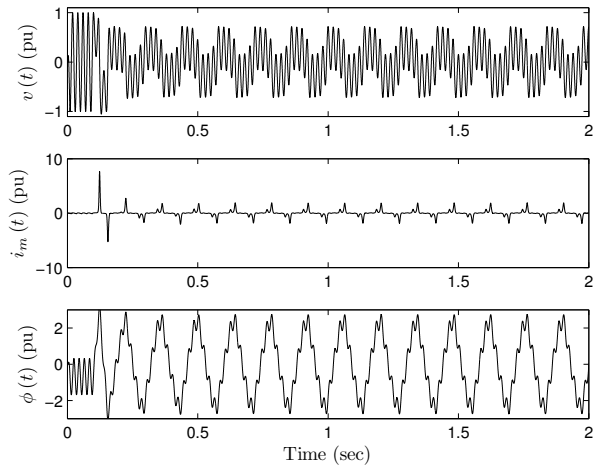

(a)

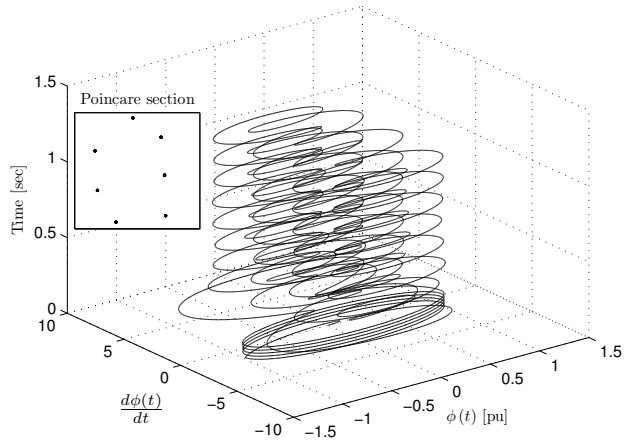

(b)

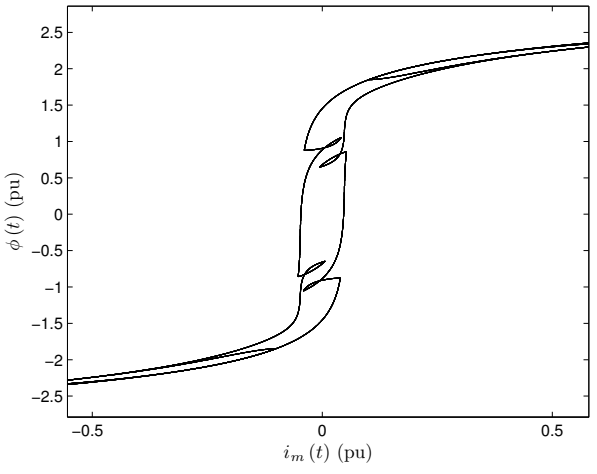

(c)

Figure 6: Subharmonic ferroresonance (Period-7) occurring at $C_{series} = 29\,\mu F$ and $C_{shunt} = 38\,\mu F$; (a) time-domain waveforms for flux, magnetizing current and voltage, (b) Poincaré and phase-plane diagrams, and (c) steady-state core hysteresis formation.

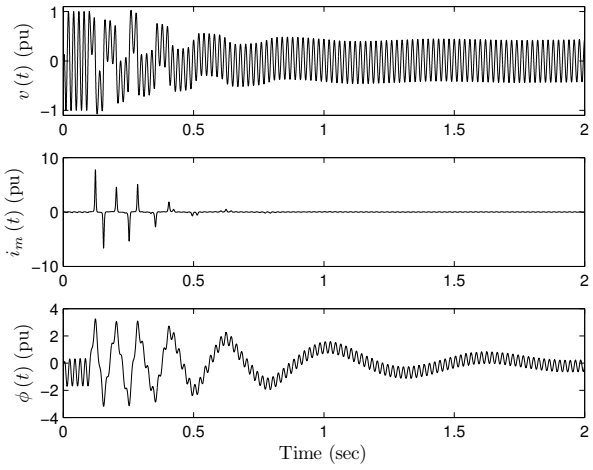

(a)

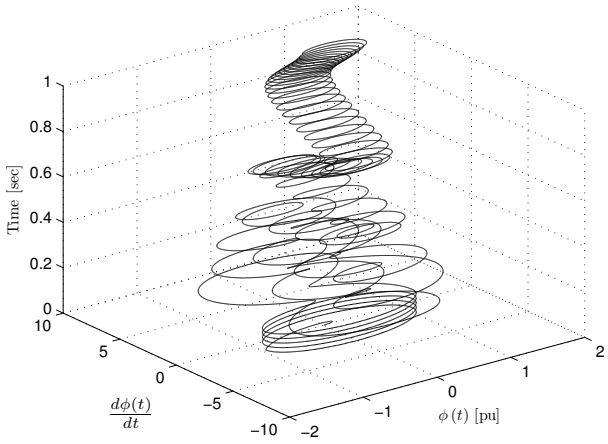

(b)

Figure 7: Temporary ferroresonance condition for $C_{series} = 28\,\mu F$ and $C_{shunt} = 38\,\mu F$. The waveforms exhibit Period-3 type ferroresonance for the first few cycles after switch is opened before dampening out; (a) time-domain waveforms for flux, magnetizing current and voltage are shown with (b) phase-plane portrait.

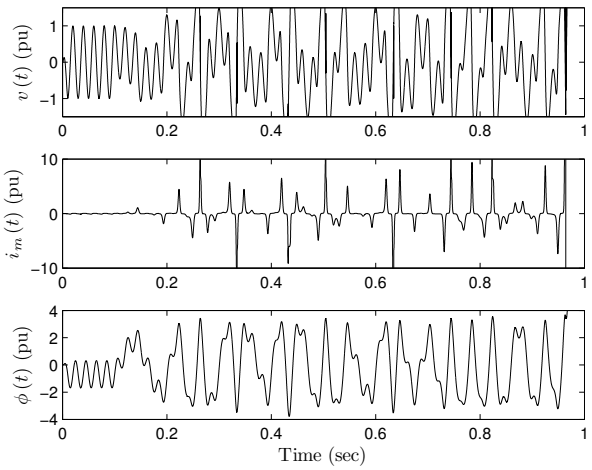

(a)

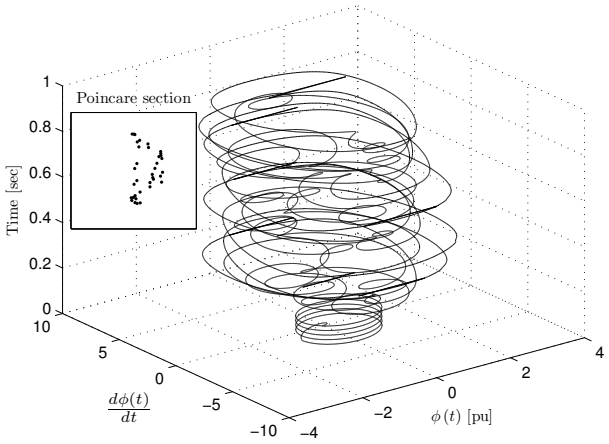

(b)

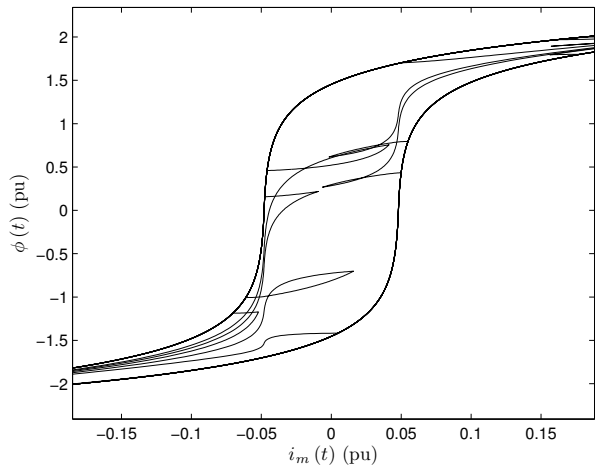

(c)

Figure 8: Chaotic ferroresonance occurring at $C_{series} = 16\,\mu F$ and $C_{shunt} = 6.4\,\mu F$; (a) time-domain waveforms for flux, magnetizing current and voltage, (b) Poincaré and phase-plane diagrams, and (c) steady-state core hysteresis formation.

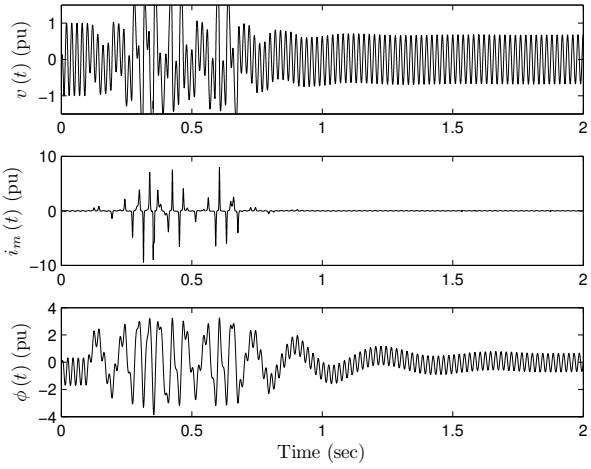

(a)

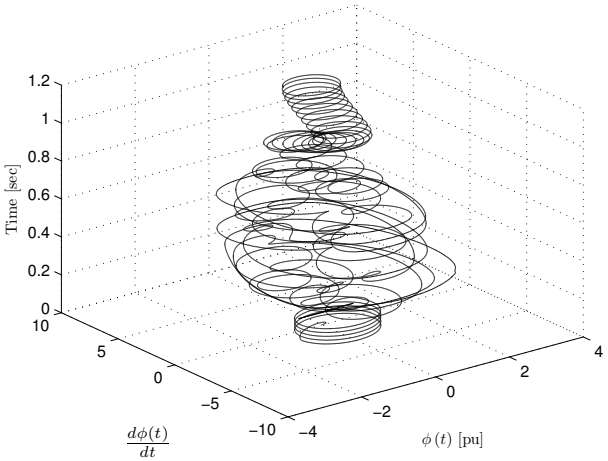

(b)

Figure 9: Temporary ferroresonance condition for $C_{series} = 16\,\mu F$ and $C_{shunt} = 8\,\mu F$. The waveforms exhibit chaotic ferroresonance modes for the first few cycles after switch is opened before dampening out; (a) time-domain waveforms for flux, magnetizing current and voltage are shown with (b) phase-plane portrait.

1 modes in the simulated scenarios, but because subharmonic modes heavily dominate the stability domain, fundamental modes may be difficult to isolate.

5.2 Chaotic Ferroresonance Modes

The most highly distorted mode of ferroresonance is the chaotic type which is aperiodic. This mode was found for C_{series} and C_{shunt} set to 16 and $6.4\,\mu F$, respectively (Fig. 8). The chaotic behavior is sustained indefinitely and is clearly illustrated by the phase-plane trajectories having non-repeating structure. The scattered Poincaré mapping also indicates the presence of a strange attractor. Very large magnetizing currents (10 pu) and overvoltages (over 1.5 pu) are observed which can thermally stress transformer core and windings and cause insulation failure. The impact on hysteresis formation under chaotic ferroresonance mode is shown in Fig. 8c where multiple minor loop trajectories are created.

Unstable chaotic modes are shown in Fig. 9 with C_{series} and C_{shunt} set to 16 and $8, \mu F$, respectively. Highly distorted chaotic ferroresonance modes similar to the previous case are observed but is only sustained for a short time before dampening out. Nevertheless, in this short time, the excessive voltage and current amplitudes can still cause permanent transformer damage.

For the studied switching scenario, generally very few chaotic ferroresonance modes were identified compared to subharmonic modes. It was also noted that under such conditions, PSPICE numerical solver sometimes failed to converge due to the highly nonlinear hysteresis equations implemented in the transformer model. Therefore, extra measures were required to complete the simulation such as decreasing the maximum step size and relaxing error tolerances.

6 Conclusion

The goal of this paper was to provide insight and a better understanding of core hysteresis behavior under dynamic conditions. Therefore, a new analysis of ferroresonance initiated by single-phase switching transients has been carried out with an improved time-domain transformer model which includes dynamic hysteresis effects of the transformer core. Several modes of ferroresonance have been identified with the developed model. A number of useful outputs such as phase-plane trajectories and Poincaré maps, as well as, core fluxes, terminal voltages and magnetizing current waveforms have been computed. The main conclusions are:

- For seemingly innocuous switching action, many subharmonic and chaotic ferroresonance modes were observed for different capacitance values which resulted in large voltage and current distortions.
- After a rigorous search, no fundamental ferroresonance modes could be recreated in this transformer model for the given switching condition. The majority of observed oscillations were subharmonic type ferroresonance modes which is consistent with the findings of [4] indicating that hysteresis leads to expanded subharmonic ferroresonance modes in the stability domain.
- Some modes of ferroresonance, especially of the chaotic type, are shown to cause severe transformer stress due to excessive terminal voltages, fluxes and magnetizing currents. Such operation can degrade winding insulation and reduce transformer life.
- The impact on the formation of minor hysteresis loops is shown for several different ferroresonance modes.
- A method for defining hysteresis nonlinearities from measurements is proposed with the use of limiting ascending and descending curve relationships and their derivative functions.
- Unlike other methods (e.g., Preisach and Jiles-Atherton approaches) which require many parameters for hysteresis to be determined experimentally, the method presented here only requires the major hysteresis loop to be measured.
- The proposed transformer model is general and can be applied to other dynamic or steady-state disturbance studies. Furthermore, the model could possibly be incorporated into large scale power system simulations to identify situations where the risk of ferroresonance is high and require mitigation strategies.
- Although the model performed admirably under extremely dynamic conditions, the convergence properties of this model can be problematic due to discontinuities created by the nonlinear hysteresis model. However, this problem is largely overcome by decreasing the maximum step size (at the expense of increasing simulation time).

References:

[1] O. Bottauscio and M. Chiampi, "Influence of hysteretic behaviour in ferroresonant LCR circuits," in *Proc. Digests of the IEEE International*

Magnetics Conference INTERMAG Asia 2005, 2005, pp. 1079–1080.

[2] B. Patel, S. Das, C. Roy, and M. Roy, "Simulation of ferroresonance with hysteresis model of transformer at no-load measured in laboratory," in *Proc. IEEE Region 10 Conference TENCON '08*, 2008, pp. 1–6.

[3] A. Rezaei-Zare, R. Iravani, and M. Sanaye-Pasand, "Impacts of transformer core hysteresis formation on stability domain of ferroresonance modes," *IEEE Trans. Power Del.*, vol. 24, no. 1, pp. 177–186, Jan. 2009.

[4] H. Lamba, M. Grinfeld, S. McKee, and R. Simpson, "Subharmonic ferroresonance in an LCR circuit with hysteresis," *IEEE Trans. Magn.*, vol. 33, no. 4, pp. 2495–2500, July 1997.

[5] M. C. Popescu, N. E. Mastorakis, C. A. Bulucea, G. Manolea, and L. Perescu-Popescu, "Nonlinear thermal model for transformers study," *WSEAS Transactions on Circuits and Systems*, vol. 8, pp. 487–497, Jun. 2009.

[6] R. C. Dugan, "Examples of ferroresonance in distribution," in *Proc. IEEE Power Engineering Society General Meeting*, vol. 2, 13–17 July 2003.

[7] D. A. N. Jacobson, "Examples of ferroresonance in a high voltage power system," in *Proc. IEEE Power Engineering Society General Meeting*, vol. 2, 13–17 July 2003.

[8] T.-P. Tsao and C.-C. Ning, "Analysis of ferroresonant overvoltages at maanshan nuclear power station in taiwan," *IEEE Trans. Power Del.*, vol. 21, no. 2, pp. 1006–1012, 2006.

[9] E. F. Fuchs and M. A. S. Masoum, *Power Quality of Electric Machines and Power Systems*. New York: Academic, 2008.

[10] M. Iravani, A. Chaudhary, W. Giesbrecht, I. Hassan, A. Keri, K. Lee, J. Martinez, A. Morched, B. Mork, M. Parniani, A. Sharshar, D. Shirmohammadi, R. Walling, and D. Woodford, "Modeling and analysis guidelines for slow transients–part III: The study of ferroresonance," *IEEE Trans. Power Del.*, vol. 15, no. 1, pp. 255–265, 2000.

[11] C. Kieny, "Application of the bifurcation theory in studying and understanding the global behavior of a ferroresonant electric power circuit," *IEEE Trans. Power Del.*, vol. 6, no. 2, pp. 866–872, 1991.

[12] B. Mork, "Ferroresonance and chaos - observation and simulation of ferroresonance in a five-legged core distribution transformer," Ph.D. dissertation, North Dakota State University, 1992.

[13] B. Mork and D. Stuehm, "Application of nonlinear dynamics and chaos to ferroresonance in distribution systems," *IEEE Trans. Power Del.*, vol. 9, no. 2, pp. 1009–1017, 1994.

[14] F. B. Amar and R. Dhifaoui, "Bifurcation diagrams and lines of period-1 ferroresonance," *WSEAS Transactions on Power Systems*, vol. 1, p. 1154, Jul. 2006.

[15] H. B. Thompson, J. M. T. Stewart, *Nonlinear dynamics and chaos: geometrical methods for engineers and scientists*. Chichester West Sussex: Wiley, 1986.

[16] J. Gleick, *Chaos: Making a New Science*. New York, NY: Viking, 1987.

[17] F. De Leon and A. Semlyen, "A simple representation of dynamic hysteresis losses in power transformers," *IEEE Trans. Power Del.*, vol. 10, no. 1, pp. 315–321, Jan. 1995.

[18] L. Chua and K. Stromsmoe, "Lumped-circuit models for nonlinear inductors exhibiting hysteresis loops," *IEEE Transactions on Circuits Theory*, vol. 17, no. 4, pp. 564–574, Nov 1970.

[19] I. D. Mayergoyz, *Mathematical models of hysteresis and their applications*, 1st ed. Elsevier, 2003.

[20] D. Jiles and D. Atherton, "Ferromagnetic hysteresis," *IEEE Trans. Magn.*, vol. 19, no. 5, pp. 2183–2185, Sep 1983.

[21] J. Tellinen, "A simple scalar model for magnetic hysteresis," *IEEE Trans. Magn.*, vol. 34, no. 4, pp. 2200–2206, 1998.

[22] M. A. Masoum and P. S. Moses, "Influence of geomagnetically induced currents on three-phase power transformers," in *Proc. Australasian Universities Power Engineering Conference AUPEC '08*, 2008, pp. 1–5.

[23] M. Masoum, P. Moses, and A. Masoum, "Derating of asymmetric three-phase transformers serving unbalanced nonlinear loads," *IEEE Trans. Power Del.*, vol. 23, no. 4, pp. 2033–2041, Oct. 2008.

[24] ——, "Impact of adjustable speed pwm drives on operation and harmonic losses of nonlinear three phase transformers," in *Proc. 7th International Conference on Power Electronics and Drive Systems PEDS '07*, 27–30 Nov. 2007, pp. 562–567.

[25] E. F. Fuchs, M. A. S. Masoum, and D. J. Roesler, "Large signal nonlinear model of anisotropic transformers for nonsinusoidal operation–part I: $\lambda - i$ characteristics," *IEEE Trans. Power Del.*, vol. 6, no. 1, pp. 1874–1886, Jan. 1991.

[26] M. A. S. Masoum, E. F. Fuchs, and D. J. Roesler, "Large signal nonlinear model of anisotropic transformers for nonsinusoidal operation–part II: Magnetizing and core-loss currents," *IEEE Trans. Power Del.*, vol. 6, no. 4, pp. 1509–1516, Oct. 1991.

[27] K. Milicevic, I. Rutnik, and I. Lukacevic, "Impact of voltage source and initial conditions on the initiation of ferroresonance," *WSEAS Transactions on Circuits and Systems*, vol. 7, pp. 800–810, Aug. 2008.